



ELSEVIER

Thermochimica Acta 332 (1999) 161–170

thermochimica  
acta

## The relaxation frequency as observed in thermally stimulated depolarisation current experiments in polymers

João F. Mano<sup>1</sup>

*Departamento de Engenharia de Polímeros, Universidade do Minho, Campus de Azurém, 4800 Guimarães, Portugal*

### Abstract

The equivalent frequency at the maximum current intensity of Debye peaks obtained by the thermally stimulated depolarisation current technique (TSDC) was discussed and its dependence on the Arrhenius parameters was calculated. The effect of the heating rate was also considered. Some specific virtual situations (zero entropy behaviour and compensation phenomena) were compared with experimental results on 11 non-conventional polymers near and below the glass transition temperature. For one such polymer, the temperature dependence on the frequency of the  $\alpha$ - and  $\beta$ -relaxation observed by dielectric relaxation spectroscopy was compared with the results obtained by thermally stimulated discharge current in the glass transition and sub- $T_g$  regions. © 1999 Elsevier Science B.V. All rights reserved.

*Keywords:* Thermally stimulated discharge current; Dielectric relaxation; Glass transition; Liquid-crystalline polymer

### 1. Introduction

The thermally stimulated depolarisation current technique (TSDC) is a dielectric related technique which is a very suitable tool for the study of the dynamics in polymeric systems [1–3]. On the other hand, the TSDC technique is one of a larger family of thermally stimulated techniques (e.g. differential scanning calorimetry, thermally stimulated creep, thermoluminescence) in which some physical property is monitored as a function of temperature during a controllable heating process. In this technique, the release current due to the depolarisation processes of a previously polarised quenched sample is measured on heating, giving the record of the complex dielectrically-active relaxation mechanisms (global experiments). One of the reported advantages of this

technique is its ability to isolate quasi-elementary processes of the complex spectra, enabling a more complete characterisation of the corresponding distribution of characteristic times (thermal sampling experiments).

In conventional dielectric or mechanical relaxation spectroscopy experiments the time scale which characterises the relaxational processes under study at a given temperature is well defined by the experimental frequency of the stimulus (periodic electric field or periodic mechanical stress, respectively) [4]. On the other hand, in thermally stimulated experiments the corresponding time scale (equivalent frequency) is intimately related to the heating rate, the relevant experimental variable in this technique.

The purpose of this work is to analyse the question of the equivalent frequency of thermally sampled peaks obtained in TSDC experiments on polymers. This will allow us to discuss some fundamental aspects of this technique and eventually to clarify

<sup>1</sup>Tel.: +351-5351-0245; fax: +351-5351-0249; e-mail: jmano@u3000.eng.uminho.pt

the differences and similarities between related techniques like TSDC and dielectric relaxation spectroscopy (or like thermally stimulated creep and mechanical relaxation spectroscopy). The discussion will be supported by previously published results obtained by TSDC in the sub- $T_g$  region and in the glass transition region of a significant set of non-conventional polymers.

## 2. Theoretical background

The dielectric relaxation behaviour of a simple Debye process can be given by

$$\tau(T)\dot{P}(t) + P(t) = P_e, \quad (1)$$

where  $P(t)$  is the polarisation of the material,  $P_e$  is the equilibrium polarisation ( $t \rightarrow \infty$ ) and  $\tau(T)$  is a characteristic time of the process which, in some cases, may be given by the Arrhenius equation:

$$\tau(T) = \tau_0 \exp(E_a/RT), \quad (2)$$

$\tau_0$  being a pre-exponential factor and  $E_a$  an apparent activation energy, or alternatively, by the Eyring equation derived from the theory of absolute rates:

$$\begin{aligned} \tau(T) &= h/kT \exp(\Delta G/RT) \\ &= h/kT \exp(-\Delta S/k) \exp(\Delta H/RT), \end{aligned} \quad (3)$$

where  $\Delta G$ ,  $\Delta S$  and  $\Delta H$  are, respectively, the activation Gibbs energy, entropy and enthalpy.

In a complex system, during isothermal polarisation at  $T=T_p$ , all dielectrically active modes at this temperature are polarised. As explained before [5], after this isothermal polarisation, in a global, as well as in a thermal sampled experiment, the sample is cooled down to  $T_0 \ll T_p$  (with the electric field applied between  $T_p$  and  $T'_p < T_p$ ). Then, the depolarisation current is measured during a constant rate heating stage ( $\beta = dT/dt$ ) up to  $T_f > T_p$ . The difference between these experiments is that in a TSDC global experiment  $T'_p = T_0$  whereas in a thermal sampling experiment  $T_p - T'_p \sim 3$  K and  $T_0 \ll T_p$ . Thus, in a thermal sampled experiment only a small set of the total accessible polarisable species is activated. Considering that in this experiment the frozen polarisation at  $T=T_0$  arose from an elementary process, the polarisation of the sample during the heating stage can be calculated

using Eq. (1), for the case  $P_e=0$ :

$$P(T) = P_0 \exp\left(-1/\beta \int_{T_0}^T dT'/\tau(T')\right), \quad (4)$$

where  $P_0$  is the total polarisation at  $t=0$  ( $T=T_0$ ). The measured current,  $J(t) = -dP(t)/dt$ , is given by

$$J(T) = \frac{P_0}{\tau(T)} \exp\left(-1/\beta \int_{T_0}^T dT'/\tau(T')\right). \quad (5)$$

This function always displays a peak-shape, and by differentiation, it is possible to write the corresponding maximum condition equation:

$$dT(T)/dT|_{T=T_m} = -\beta^{-1}, \quad (6)$$

where  $T_m$  is the temperature of maximum current intensity. The relaxation frequency (or equivalent frequency) of the experiment,  $f_m$ , may be defined as the characteristic frequency at  $T=T_m$ :

$$f_m = 1/2\pi\tau_m, \quad (7)$$

where  $\tau_m = \tau(T_m)$  is the relaxation time at the temperature of maximum current intensity (or at the inflexion point of the  $P(T)$  curve).

Considering that the relaxation time of the elementary processes follows a simple Arrhenius' relationship, Eqs. (2) and (6) can be rewritten respectively as

$$\tau_m = \begin{cases} \tau_0 \exp(E_a/RT_m), \\ RT_m^2/\beta E_a, \end{cases} \quad (8)$$

In Eq. (8) we thus have two equations and four variables:  $\tau_m$  (or  $f_m$ ),  $T_m$ ,  $E_a$  and  $\tau_0$ . The thermokinetic parameters of a thermal sampled peak,  $E_a$  and  $\tau_0$ , can be calculated by fitting  $\tau(T)$  with the Arrhenius equation. The temperature dependence of the relaxation time ( $\tau(T)$ ) can, on the other hand, be obtained by applying the so-called BFG treatment [6] to the ascending side of the peak:

$$\ln\tau(T) = \ln[P(T)/J(T)] = \ln \int_T^\infty J(t)dt - \ln J(T). \quad (9)$$

Thus, using Eq. (8), both the dependence of  $T_m$  and  $\tau_m$  (or  $f_m$ ) on the independent pair of variables ( $E_a$ ,  $\log\tau_0$ )

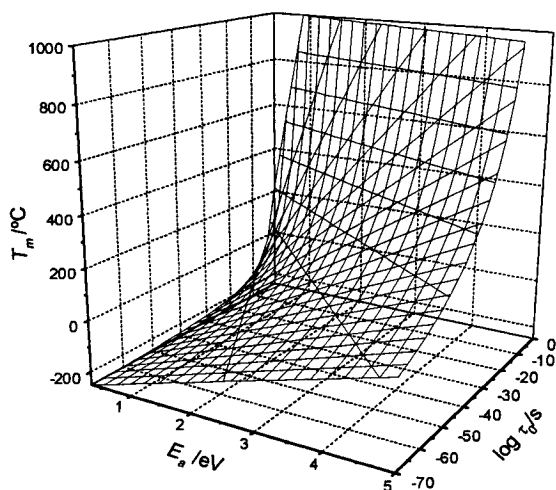


Fig. 1. Theoretical prediction of the temperature of maximum intensity for elementary TSDC peaks as a function of the Arrhenius parameters (heating rate of  $4 \text{ K min}^{-1}$ ).

can be obtained. The variation of  $T_m$  and  $\log f_m$  within a large range of  $E_a$  and  $\tau_0$  values, which are usually observed in experimental data, are shown in Fig. 1–Fig. 2, respectively, for a heating rate of  $4 \text{ K min}^{-1}$ . The experimental points shown in Fig. 2 will be discussed later.

The surface plot shown in Fig. 1 suggests that the temperature of maximum intensity of an elementary peak is very sensitive to the thermokinetic parameters and increases, as expected, with the increase of both  $E_a$  and  $\log \tau_0$ . It must be pointed out that in usual experimental results, the thermokinetic parameters do not fill all the  $(E_a, \log \tau_0)$  space shown in Fig. 2. In fact, it has been observed in TSDC studies on a wide variety of materials (some of those results will be presented in this paper) that the  $(E_a, \log \tau_0)$  values accessible in this technique are such that  $\log f_m$  is usually between  $-2$  and  $-3$  for a heating rate of  $4 \text{ K min}^{-1}$ . These frequencies are low compared with those commonly used in dynamical dielectric and mechanical experiments.

### 3. Discussion

The time scale of the thermal sampled peaks in the low temperature region, as well as in the glass transition region, will be discussed for the 11 polymers presented in Table 1. These polymers show liquid-

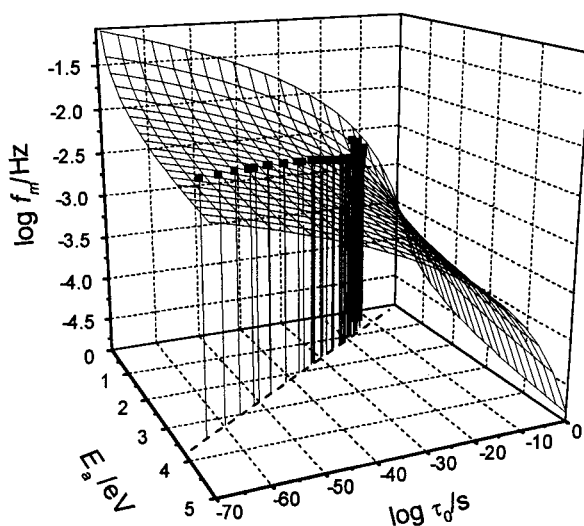


Fig. 2. Theoretical prediction of the equivalent frequency for elementary TSDC peaks as a function of the Arrhenius parameters (heating rate of  $4 \text{ K min}^{-1}$ ). Symbols: equivalent frequency of some thermal sampled peaks of LCP1 obtained in the sub- $T_g$  and in the glass transition regions at  $4 \text{ K min}^{-1}$ . Dashed line: compensation line observed for the points corresponding to the glass transition relaxation of LCP1.

crystalline character above  $T_g$  up to a clearing temperature due to the presence of the mesogenic moiety in the side group of the repetitive units. This class of materials has been widely investigated over the last 20 years because of their interesting electro-optical properties combined with many physical properties of conventional polymers [7,8]. The transition temperatures of these polymers,  $T_{tr}$ , are also shown in Table 1.

All the polymers in Table 1 have been studied by TSDC [9–17] and it was found that they show relaxational processes below  $T_g$ , near the glass transition region and above the glass transition temperature (one or two relaxations in the liquid-crystalline phase); these upper  $T_g$  relaxations will not be considered here.

We first focus on the equivalent frequency for LCP1. It was observed previously [9] that this polymer has a low temperature relaxation (the corresponding sampled peaks were observed between  $-150^\circ\text{C}$  up to  $\approx -50^\circ\text{C}$ ) and a relaxation, between  $\approx -50^\circ\text{C}$  and  $\approx 0^\circ\text{C}$ , ascribed to the dynamic glass transition. By using the BFG equation, the corresponding thermokinetic parameters were obtained for each thermal sampled peak. In Fig. 3 the relaxation time of some peaks in the glass transition region, calculated from

Table 1

Code name, structure and transition temperatures ( $T_{tr}$ ) of the investigated polymers (phases: g-glass; N-nematic; S<sub>a</sub>-smectic-A; S<sub>c</sub>-smectic-C; I-isotropic)

Name	Structure	$T_{tr}$ (°C)
LCP 1		g-7,2 S <sub>c</sub> 76,8 I
LCP 83		g 37,2 S <sub>a</sub> 148,6 I
LCP 18		g 20 S <sub>a</sub> 129 I
LCP 93		g -3,9 S <sub>a</sub> 79,1 I
HOM		g 5 S <sub>a</sub> 95 I
COP		g -15 S <sub>a</sub> 57 I
LCP 95		g 46,7 S <sub>a</sub> 82,9 I
LCP 105		g 38 N 127 I
LCP 100		g 75 N 111 I
LCP 92		g 61,5 N 113,4 I
LCP 94		g 39,0 S <sub>a</sub> 127,5 I

The experimental details and the extended discussion of the results can be found in [9–17].

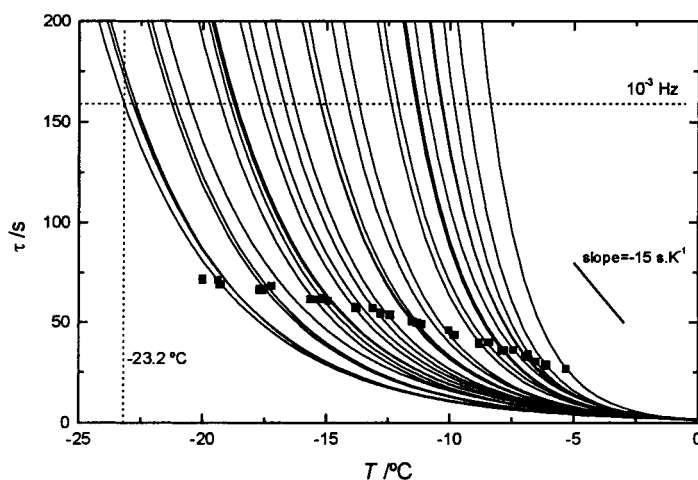


Fig. 3. Arrhenius lines of some sampled peaks of LCPI in the glass transition. Symbols: relaxation time at the maximum current temperature as a function of  $T_m$  for the same peaks calculated with the second equation in expression (8).

the Arrhenius equation, is plotted as a function of temperature (solid lines). The left hand-side line corresponds to a thermal sampled peak obtained with  $T_p = -33^\circ\text{C}$  ( $T_m = -22^\circ\text{C}$ ) and the right hand-side one was obtained with  $T_p = -8^\circ\text{C}$  ( $T_m = -5.3^\circ\text{C}$ ).

The square points in Fig. 3 represent the relaxation time at  $T = T_m$ ,  $\tau_m$ , calculated according to the maximum condition for each sampled peak (second equation of (8)), as a function of the experimental  $T_m$ . It is clear from that figure that, in the glass transition region,  $\tau_m$  decreases with increasing  $T_m$  (or  $T_p$ ). This means that the equivalent frequency depends on the elementary process, for the same heating rate.

It is interesting to compare this TSDC feature with that expected in dielectric relaxation experiments, isothermal and isochronal. Consider an elementary process studied by dielectric relaxation. If the experiment is isothermal, the frequency is scanned so that the time scale of the sample is constant (constant temperature and pressure) and the time scale of the experiment is changing. In an isochronal experiment, on the other hand, the frequency is constant and the temperature changes at a given rate so that the experimental time scale is constant and, due to the heating, the relaxation time of the sample is being reduced. In both cases the dielectric relaxation peak will occur when the two time scales, that of sample and that of the experiment, intersect. As pointed out before, and opposite to the isochronal dielectric relaxation experi-

ment where the experimental frequency is constant, in TSDC the characteristic frequency is not constant for a given heating rate; see, in Fig. 3, that  $\tau_m$  decreases with increasing  $T_m$ . In fact, the maximum intensity of a TSDC peak does not occur at the intersection of the two time scales, as in dielectric relaxation experiments, but rather in a situation where the rate of decrease of the relaxation time with increasing temperature becomes equal to the reciprocal of the experimental heating rate (see Eq. (6)). For example, for an experiment with a heating rate of  $4\text{ K min}^{-1}$ , the maximum of the TSDC peak will occur at a temperature such that the slope of the  $\tau(T)$  curve is  $-15\text{ s K}^{-1}$  (see Fig. 3). Since the slope of the  $\tau(T)$  curves for elementary processes in the glass transition region increases as  $T_m$  increases, as a consequence of the so-called compensation behaviour, the condition where this slope is  $-15\text{ s K}^{-1}$  corresponds to values of  $\tau_m$  which decrease with increasing  $T_m$ .

The type of representation shown in Fig. 3 may help us to analyse the dependence of  $\tau_m$  and  $T_m$  on the heating rate. The increase of the heating rate decreases the absolute value of the slope of the  $\tau$  versus  $T$  line at which the maximum current occurs. Thus, the temperature of maximum intensity is shifted to higher  $T_m$  and  $\tau_m$  decreases (or  $f_m$  increases). In Fig. 4, the expected  $T_m$  and  $f_m$  values for the sampled peak at lower temperature of Fig. 3, calculated with Eqs. (7) and (8), are presented in an Arrhenius plot ( $\log f$  versus

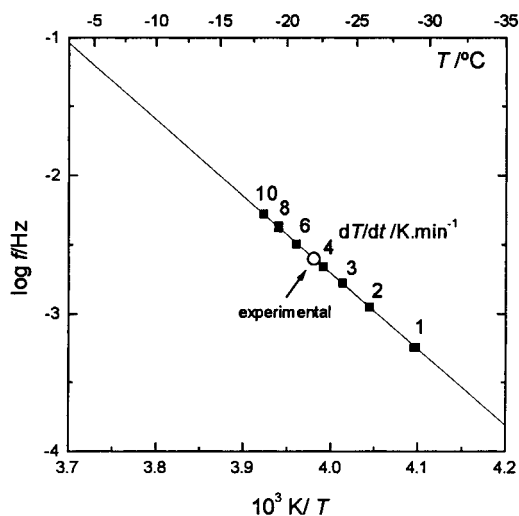


Fig. 4. Solid line: Arrhenius line calculated with the thermokinetic parameters of a sampled peak of LCPI, corresponding to the lowest temperature line in Fig. 3. Square symbols: predicted  $f_m$  and  $T_m$  for the different heating rates shown. Circle: experimental point obtained at  $4 \text{ K min}^{-1}$ .

$10^3/T$ ) for  $\beta$  from 1 to  $10 \text{ K min}^{-1}$ . It can be concluded that the increase of  $T_m$  or  $\log f_m$  becomes smaller as the heating rate increases. The experimental point obtained at  $4 \text{ K min}^{-1}$  is also shown in the figure (open circle).

### 3.1. Temperature dependence of the relaxation frequency

The equivalent frequency of the thermal sampled peaks of the analysed polymers is shown in Fig. 5 as a function of  $T_m$ , covering the low temperature relaxation and the glass transition relaxation. It is clear from this figure that, for the low temperature relaxation of all materials, corresponding to the peaks with  $T_m$  below  $\approx -50^\circ\text{C}$ , the equivalent frequency smoothly decreases around  $0.0025 \text{ Hz}$  with increasing  $T_m$ . This “universal” behaviour observed for these sub- $T_g$  relaxations will be discussed below. On the other hand, in the glass transition region a strong increase of  $f_m$  is observed as the temperature approaches  $T_g$ . This dramatic change is also observed for the activation enthalpy (or  $E_a$ ) and activation entropy [18] due to the increase of the complexity of the molecular motions involved during the approximation, from

the low temperature side, of the glass transition temperature.

The activation entropies,  $\Delta S$ , of the thermal sampled peaks of the sub- $T_g$  processes were found to be negligible. This behaviour has been usually found in local and non-cooperative processes [19,20]. From the Eyring equation, it can be shown that the  $\Delta S=0$  behaviour (that is,  $\Delta G=\Delta H$ ) leads to the following equality, which may be applied to TSDC results [21,22]:

$$\begin{aligned} E_a &= RT_m[1 + \ln(k/h) + \ln(T_m\tau_m)] \\ &= RT_m[22.92 + \ln(T_m/f_m)]. \end{aligned} \quad (10)$$

Eq. (10) is independent of the equations in expression (8). Therefore, when  $\Delta S=0$ , we have a set of three equations and four variables, and consequently, it is possible to have access to a dependence of any three variables on a fourth one. Considering  $T_m$  as the independent variable we can predict the corresponding evolution of  $f_m$  (or  $\tau_m$ ). This prediction is shown in Fig. 5 for the temperature range take over  $-160^\circ\text{C}$  to  $0^\circ\text{C}$ . It can be concluded that this prediction is consistent with the data at low temperatures, where  $\Delta S \approx 0$ .

It would be interesting to predict the evolution of  $f_m$  with  $T_m$  in the glass transition region. Obviously, in this case, the  $\Delta S=0$  behaviour is no longer observed; thus, Eq. (10) cannot be applied. However, it is known that in this region a linear relationship between  $E_a$  and  $\log\tau_0$  (or between  $\Delta H$  and  $\Delta S$ ) is observed:

$$\log\tau_0 = \log\tau_c - \frac{E_a}{\ln(10)RT_c}. \quad (11)$$

This behaviour is usually called *compensation phenomena* and the two compensation parameters in Eq. (11),  $\tau_c$  and  $T_c$  (compensation time and temperature), are fixed for one material. Thus, knowing these two parameters, we have again a third equation and the expected dependence of  $f_m$  with  $T_m$  can be calculated. The compensation parameters of LCPI were found to be  $\tau_c=2.0 \text{ s}$  and  $T_c=-0.7^\circ\text{C}$  [9]. The expected dependence of the equivalent frequency on  $T_m$  in the glass transition region of LCPI is also shown in Fig. 5. Here, there is an excellent agreement between this calculated dependence and the experimental points (squares) in the temperature range between  $-20^\circ\text{C}$  and  $-5^\circ\text{C}$ , where the compensation behaviour is nearly perfect. However, below  $\approx -20^\circ\text{C}$ , calculated

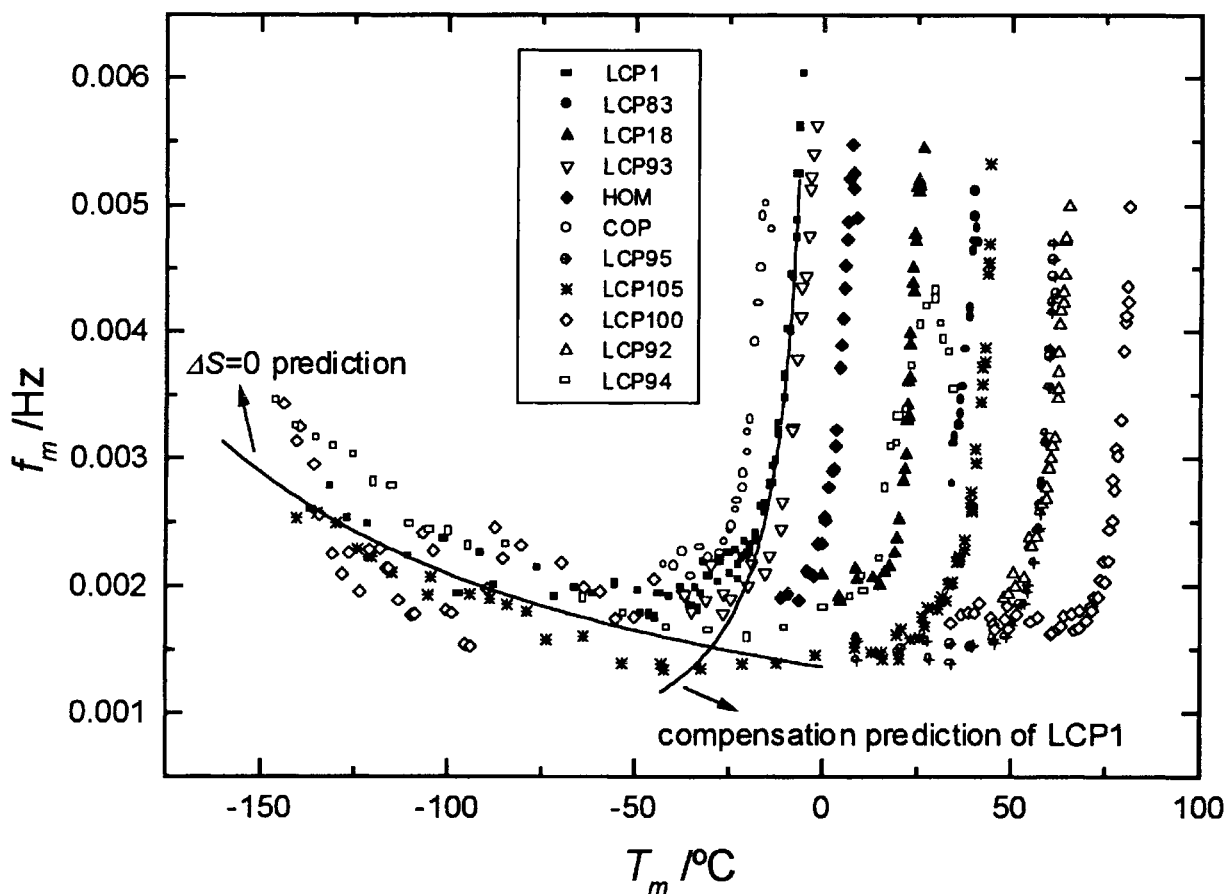


Fig. 5. Equivalent frequency as a function of the temperature of maximum intensity for the thermal sampled peaks of the 11 analysed polymers near and below the glass transition temperature. The solid lines are predictions for the case of a general zero-entropy behaviour and for LCP1 in the glass transition region assuming a compensation relationship.

values diverge from the experimental data because the system no longer follows the compensation phenomena. This kind of behaviour can also be observed when attempts are made to predict the evolution of the activation energy with  $T_m$  in the glass transition region [15]. It must be said that, despite being real and observable, some authors consider that the compensation phenomena may be a consequence of mathematical artefacts and it is difficult to give a physical meaning of the compensation parameters. However, one can conclude that these parameters may be used in order to predict some important variables in a temperature region where compensation phenomena is observed. The equivalent frequency of the thermal sampled peaks of LCP1 below  $T_g$  is also shown in

Fig. 2 (square points) in terms of its dependence on the thermokinetic parameters,  $E_a$ , and  $\log\tau_0$ . All the experimental points are in good agreement with the theoretical prediction based on expression (8) (surface plot in the figure). The points with  $E_a < 20 \text{ kcal mol}^{-1}$  correspond to the thermal sampled peaks of the low temperature relaxation. The higher energy points are related to the glass transition relaxation. From the projections of these points on the  $(E_a, \log\tau_0)$  plane the compensation behaviour can be recognised (see dashed line in Fig. 2): the slope of  $\log\tau_0$  versus  $E_a$  is proportional to  $T_c^{-1}$  and the intercept (when  $E_a \rightarrow 0$ ) is  $\log\tau_c$  (see Eq. (11)). The increase of  $E_a$  corresponds to an increase of  $T_m$  and, as was observed in Fig. 5, the equivalent frequency of the processes increases when

the approximation to  $T_g$  is made from the low temperature side.

### 3.2. Comparison between TSDC and dielectric relaxation spectroscopy results

The comparison of the time scale of relaxation processes when investigated by dielectric relaxation spectroscopy or by TSDC (or dynamical mechanical analysis and thermally stimulated creep) has been tried by some authors [22–27]. For this, one should use TSDC global spectra because, in dielectric relaxation spectroscopy, it is not possible to experimentally decompose the complex behaviour of the relaxations into elementary processes. However, it is difficult to calculate an equivalent frequency of a global TSDC peak because of the uncertainty of the mean thermokinetic values when calculated by the usual methods. In fact, such methods are valid only for elementary processes.

Dielectric relaxation spectroscopy studies were previously carried out for LCPI, in the frequency range from  $10^{-2}$  to  $10^6$  Hz [9]. As usually observed in side-chain liquid crystal polymers, two relaxation processes were detected in the liquid-crystalline phase: the  $\delta$ -relaxation and, at lower frequencies, the  $\alpha$ -relaxation. The origin of the  $\alpha$ -relaxation observed in side-chain liquid crystal polymers at the molecular level is controversial. Some authors believe that this process is equivalent to the  $\alpha$ -relaxation found in conventional amorphous polymers (dynamic glass transition) [28–32]. However, some other investigators have attributed this process to special conformational rearrangements within the side-chains (molecular motions mainly involving the transverse component of the dipole moment of the mesogenic groups) [33–41]. In this context, a comparison of the  $\alpha$ -relaxation observed by dielectric relaxation spectroscopy and the glass transition relaxation observed by TSDC would be particularly interesting for such materials. In fact, we know that the glass transition relaxation of these materials observed by TSDC corresponds to the usual  $\alpha$ -relaxation observed in conventional polymers.

The frequency at the maximum of the loss peak of the  $\alpha$ -relaxation of LCPI is plotted against reciprocal temperature in Fig. 6 (circles). This also shows the corresponding fit according to the Vogel–Fulcher

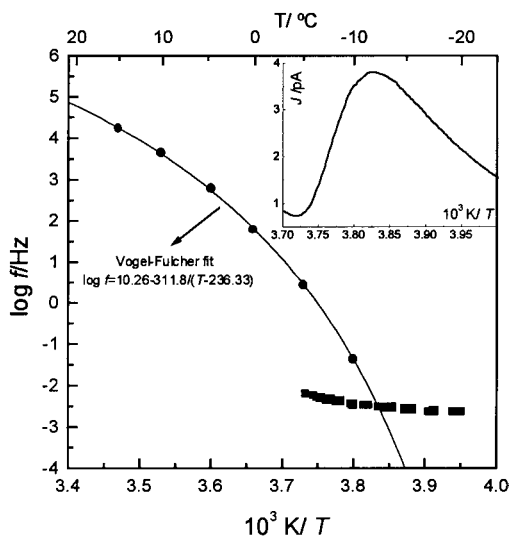


Fig. 6. Comparison of dielectric results (circles) corresponding to the  $\alpha$ -relaxation and TSDC results (thermal sampled experiments) in the glass transition region (squares) for LCPI. Insert: global TSDC spectrum of LCPI in the glass transition region; the temperature axis is the same as for the main graphics.

equation,  $\tau(T) = \tau_\infty \exp[B/(T - T_0)]$ . The TSDC relaxation plot ( $\log f_m$  versus  $1000/T_m$ ) for a set of sampled peaks in the glass transition region, with  $T_m$  between  $-20^\circ\text{C}$  and  $-5^\circ\text{C}$ , is also shown in Fig. 6. Extrapolation of the dielectric relaxation spectroscopy results to low frequencies intercepts the TSDC data at  $\approx -12^\circ\text{C}$ . This temperature is right in the temperature range of the sampled TSDC peaks. The insert in Fig. 6 shows the global spectrum of LCPI in this temperature region also obtained at  $4 \text{ K min}^{-1}$  (see [9] for details). It is interesting to note that the maximum current temperature of this complex peak is very close to the intersection temperature of the relaxation plot obtained by dielectric relaxation spectroscopy and thermal sampling experiments. It can be concluded that the underlying processes in the  $\alpha$ -relaxation observed by dielectric relaxation spectroscopy, and in the glass transition relaxation observed by TSDC, are very similar. Therefore, we may be tempted to assign the  $\alpha$ -relaxation to the glass transition process, for the case of LCPI. The study of the structural relaxation of LCPI by differential scanning calorimetry also allowed the calculation of the temperature dependence of the mean relaxation time in the glass transition region [42]. Comparison of these results



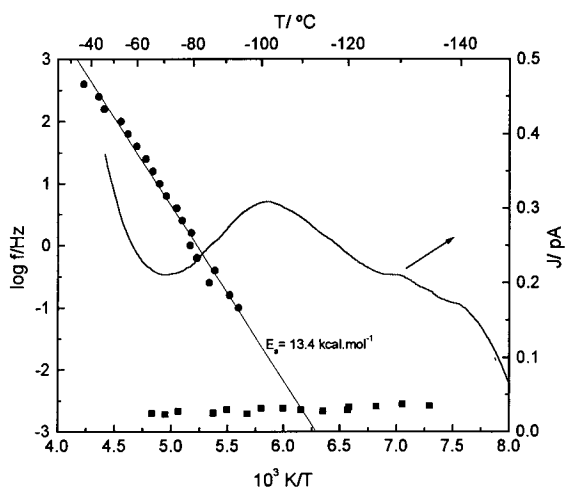


Fig. 7. Comparison of dielectric results (circles) corresponding to the  $\beta$ -relaxation and TSDC results (thermal sampled experiments) for the sub- $T_g$  region (squares) of LCPI. The solid line represents the global TSDC spectrum in the sub- $T_g$  region (see [9] for experimental details).

with the dielectric relaxation spectroscopy data seems to strengthen the case for an origin in the  $\alpha$ -relaxation.

The comparison of the data obtained by both dielectric techniques may also be applied to the sub- $T_g$  relaxation. In Fig. 7 the dielectric relaxation spectroscopy results (square points) suggests, as shown before [9], an Arrhenius behaviour. The solid line in Fig. 7 corresponds to the global spectrum of LCPI on the low temperature relaxation region. It can be seen that the sub-glass process is very broad, covering the temperature range from  $-140^\circ\text{C}$  to  $-70^\circ\text{C}$  (above  $\approx -70^\circ\text{C}$  the glass transition temperature relaxation starts to emerge). It was suggested that two different modes of molecular motions could be involved in this process [43]. The square points represent the frequency dependence on  $T_m$  for sampled peaks in this temperature region. The extrapolation of the dielectric results to lower frequencies intercepts the TSDC data at  $\approx -110^\circ\text{C}$ , in the temperature range of both the TSDC sampled results and the global spectrum. The results show that the molecular motions involved in the  $\beta$ -relaxation observed by dielectric relaxation spectroscopy and in the sub- $T_g$  relaxation observed by TSDC are very similar and confirm that the two techniques are complementary.

#### 4. Conclusions

The dependence of both temperature of maximum intensity ( $T_m$ ) and equivalent frequency ( $f_m$ ) on the Arrhenius parameters in thermal sampled peaks was calculated for a fixed heating rate ( $4\text{ K min}^{-1}$ ). Predictions were shown to be compatible with experimental results for one polymer in the glass transition and in the low temperature region.

It was shown that the equivalent frequency variation for a series of thermal sampled peaks depends on the process under study: for 11 polymers it was observed that in the low temperature region,  $f_m$  decreases smoothly with temperature; on the other hand, in the glass transition region a stronger increase of  $f_m$  is detected. Nevertheless, for all analysed polymers, the frequency was found to be in the range  $0.001$ – $0.006\text{ Hz}$ .

An universal prediction of the evolution of the frequency with temperature for non-cooperative relaxations was obtained without any adjustable parameters. The calculations were shown to be compatible with the experimental results in the low temperature relaxation for the investigated polymers. It was shown that the expected  $f_m(T_m)$  evolution in the glass transition region, where the compensation phenomena is observed, may also be calculated provided that the compensation parameters are given.

The Arrhenius map of the  $\alpha$ -relaxation of one polymer studied by dielectric relaxation spectroscopy was found to be consistent with the time scale of the thermal sampled peaks of the glass transition relaxation as studied by TSDC. The same consistency was also observed for the sub-glass relaxation.

#### Acknowledgements

The author would like to thank Prof. J.J. Moura Ramos (Technical University of Lisbon) for his useful discussions.

#### References

- [1] J. van Turnhout, Thermally Stimulated Discharges of Polymer Electrets, Elsevier, Amsterdam, 1975.
- [2] R. Chen, Y. Krish, Analysis of Thermally Stimulated Processes, Pergamon Press, Oxford, 1981.

- [3] S.H. Carr, Thermally stimulated discharge current analysis of polymers, in: E.A. Seanor (Ed.), *Electric Properties of Polymers*, Academic Press, New York, 1982.
- [4] N.G. McCrum, B.E. Read, G. Williams, *Anelastic and Dielectric Effects in Polymer Solids*, Dover, New York, 1991.
- [5] A.B. Dias, N.T. Correia, J.J. Moura Ramos, A.C. Fernandes, *Polym. Int.* 33 (1994) 293.
- [6] C. Bucci, R. Fieschi, G. Guidi, *Phys. Rev.* 148 (1966) 816.
- [7] C.B. McArdle (Ed.), *Side Chain Liquid Crystalline Polymers*, Blackie, Glasgow, 1989.
- [8] A.N. Donald, A.H. Windle, *Liquid-Crystalline Polymers*, Cambridge University Press, Cambridge, 1992.
- [9] J.F. Mano, N.T. Correia, J.J. Moura Ramos, S. Andrews, G. Williams, *Liq. Cryst.* 20 (1996) 201.
- [10] J.F. Mano, N.T. Correia, J.J. Moura Ramos, A.C. Fernandes, *J. Polym. Sci., Polym. Phys. Ed.* 33 (1995) 269.
- [11] J.F. Mano, J.J. Moura Ramos, D. Lacey, *Polymer* 37 (1996) 3161.
- [12] J.F. Mano, J.J. Moura Ramos, *J. Thermal Anal.* 44 (1995) 1037.
- [13] J.J. Moura Ramos, J.F. Mano, D. Lacey, G. Nestor, *J. Polym. Sci., Polym. Phys. Ed.* 34 (1996) 2067.
- [14] J.F. Mano, J.J. Moura Ramos, A.C. Fernandes, G. Williams, *Polymer* 35 (1994) 5170.
- [15] J.J. Moura Ramos, J.F. Mano, *Thermochim. Acta* 285 (1996) 347.
- [16] J.J. Moura Ramos, J.F. Mano, D. Coates, *Mol. Cryst. Liq. Cryst.* 281 (1996) 267.
- [17] J.F. Mano, N.T. Correia, J.J. Moura Ramos, D. Coates, *Macromol. Chem. Phys.* 196 (1995) 2289.
- [18] J.J. Moura Ramos, J.F. Mano, B.B. Sauer, *Polymer* 38 (1997) 1081.
- [19] H. Starkweather Jr., *Macromolecules* 14 (1981) 1277.
- [20] H. Starkweather Jr., *Macromolecules* 21 (1988) 1798.
- [21] B.B. Sauer, P. Avakian, H. Starkweather Jr., B.S. Hsiao, *Macromolecules* 23 (1990) 5119.
- [22] B.B. Sauer, P. Avakian, *Polymer* 33 (1992) 5128.
- [23] B.E. Read, *Polymer* 30 (1989) 1439.
- [24] J.J. Moura Ramos, R.C. Sousa, N.T. Correia, M. Dionísio, *Ber. Bunsenges. Phys. Chem.* 100 (1996) 571.
- [25] M. Grimau, E. Laredo, A. Bello, N. Suarez, *J. Polym. Sci., Polym. Phys. Ed.* 35 (1997) 2483.
- [26] R. Pelster, T. Kruse, H.G. Krauthäuser, G. Nimtz, P. Pissis, *Phys. Rev. B* 57 (1998) 8763.
- [27] R. Pelster, T. Kruse, H.G. Krauthäuser, V. Grunow, G. Nimtz, P. Pissis, *J. Non-Cryst. Solids* 160 (1998) 235–237.
- [28] R. Zentel, G.R. Strobl, H. Ringsdorf, *Macromolecules* 18 (1985) 960.
- [29] F. Kremer, S.U. Vallerien, R. Zentel, H. Kapitza, *Macromolecules* 22 (1989) 4040.
- [30] F.R. Colomer, J.M. Meseguer Dueñas, J.L. Gómez Ribelles, J.M. Barrales-Rienda, J.M. Bautista de Ojeda, *Macromolecules* 26 (1993) 155.
- [31] U.W. Gedde, F. Liu, A. Hult, F. Sahlen, R.H. Boyd, *Polymer* 35 (1994) 2056.
- [32] A. Schönhal, U. Geßner, J. Rübner, *Macromol. Chem. Phys.* 196 (1995) 1671.
- [33] G.S. Attard, G. Williams, *Polym. Commun.* 27 (1986) 2.
- [34] G.S. Attard, G. Williams, *Liq. Cryst.* 1 (1986) 253.
- [35] G.S. Attard, G. Williams, G.W. Gray, D. Lacey, P.A. Gemmel, *Polymer* 27 (1986) 185.
- [36] G. Williams, *Polymer* 35 (1994) 1915 references therein.
- [37] S.R. Andrews, G. Williams, L. Läsker, J. Stumpe, *Macromolecules* 28 (1995) 8463.
- [38] H. Seiberle, W. Stille, G. Strobl, *Macromolecules* 23 (1990) 2008.
- [39] Z.Z. Zhong, D.E. Schuele, S.W. Smith, W.L. Gordon, *Macromolecules* 26 (1993) 6403.
- [40] Z.Z. Zhong, W.L. Gordon, D.E. Schuele, R.B. Akins, V. Percec, *Mol. Cryst. Liq. Cryst.* 238 (1994) 129.
- [41] Z.Z. Zhong, D.E. Schuele, W.L. Gordon, *Liq. Cryst.* 17 (1994) 199.
- [42] J.F. Mano, N.M. Alves, J.M. Meseguer Dueñas, J.L. Gómez Ribelles, *Polymer*, in press.
- [43] J.F. Mano, J.J. Moura Ramos, *Thermochim. Acta* 323 (1998) 65.